Icarus 318 (2019) 205–211

Contents lists available at ScienceDirect

Icarus

journal homepage: www.elsevier.com/locate/icarus

Mineralogy of the Occator quadrangle

A. Longobardo[a,*], E. Palomba[a,b], F.G. Carrozzo[a], A. Galiano[a], M.C. De Sanctis[a], K. Stephan[c], F. Tosi[a], A. Raponi[a], M. Ciarniello[a], F. Zambon[a], A. Frigeri[a], E. Ammannito[d], C.A. Raymond[e], C.T. Russell[f]

[a] INAF-IAPS, via Fosso del Cavaliere 100, I-00133 Rome, Italy
[b] ASI-ASDC, via del Politecnico snc, I-00133 Rome, Italy
[c] Institute for Planetary Research, Deutsches Zentrum fur Luft- und Raumfahrt (DLR), D-12489 Berlin, Germany
[d] ASI-URS, via del Politecnico snc, I-00133 Rome, Italy
[e] California Institute of Technology, JPL, 91109 Pasadena, CA, USA
[f] UCLA, Los Angeles, CA 90095, USA

ARTICLE INFO

Article history:
Received 28 April 2017
Revised 11 September 2017
Accepted 18 September 2017
Available online 22 September 2017

Keywords:
Asteroid ceres
Asteroids
Spectroscopy

ABSTRACT

We present an analysis of the areal distribution of spectral parameters derived from the VIR imaging spectrometer on board NASA/Dawn spacecraft. Specifically we studied the Occator quadrangle of Ceres, which is bounded by latitudes 22°S to 22°N and longitudes 214°E to 288°E, as part of the overall study of Ceres' surface composition reported in this special publication. The spectral parameters used are the photometrically corrected reflectance at 1.2 μm, the infrared spectral slope (1.1–1.9 μm), and depths of the absorption bands at 2.7 μm and 3.1 μm that are ascribed to hydrated and ammoniated materials, respectively.

We find an overall correlation between 2.7 μm and 3.1 μm band depths, in agreement with Ceres global behavior, and band depths are shallower and the spectral slope is flatter for younger craters, probably due to physical properties of regolith such as grain size. Spectral variations correlated with the tali geological unit also suggest differences in physical properties. The deepest band, indicating enrichment of ammoniated phyllosilicates, are associated with ejecta generated by impacts that occurred in southern quadrangles.

The most peculiar region of this quadrangle is the Occator crater (20°N 240°E). The internal crater area contains two faculae, which are the brightest areas on Ceres due to exposure of sodium carbonates, and by two types of ejecta, dark and bright, with different spectral properties, probably due to different formation, evolution or age.

1. Introduction

The Dawn/NASA mission is orbiting around Ceres since April 2015 (Russell and Raymond, 2011), and is taking color and hyperspectral images by means of the Framing Camera (FC) (Sierks et al., 2011) and the Visual and InfraRed spectrometer (VIR) (De Sanctis et al., 2011).

Dawn revealed a homogeneously dark body, with an average reflectance at standard geometry (incidence and phase angle of 30°, emission angle 0°) of 0.03 at 0.55 μm (Ciarniello et al., 2017; Longobardo et al., 2017a). However, many bright spots are found on its surface (Stein et al., 2017; Palomba et al., 2017). The brightest ones, i.e. Cerealia and Vinalia Faculae (Stein et al., 2017; De Sanctis et al., 2016), are observed in the Occator crater (20°N, 240°E): their 0.55 μm reflectance at standard geometry reaches values up to 0.26 (De Sanctis et al. 2016).

Ceres' surface composition is quite homogeneous, and consists of a mixture of ammoniated phyllosilicates, Mg-carbonates and dark materials (De Sanctis et al., 2015). The absorption bands associated with these materials, as revealed by the VIR spectrometer, are centered at 2.7 μm (related to phyllosilicates), 3.1 μm (due to NH_4), 3.4 μm and 4.0 μm, both due to carbonates (De Sanctis et al. 2015, 2016); dark materials are instead spectrally featureless. Ammannito et al. (2016) showed a moderate correlation between band depths at 2.7 μm and 3.1 μm, indicating a widespread distribution of ammoniated phyllosilicates. As suggested by distribution of band depths, the abundance of these components is higher in the Southern Hemisphere and in the part of the equatorial region centered on the Kerwan crater (10°S, 123°E).

* Corresponding author.
E-mail address: andrea.longobardo@iaps.inaf.it (A. Longobardo).

https://doi.org/10.1016/j.icarus.2017.09.022
0019-1035/

Some localized regions show deepening of bands at 3.4 μm and 4.0 μm, which has been interpreted as carbonate enrichments (De Sanctis et al., 2016; Carrozzo et al., 2017). Moreover, the longward band center shift of these bands indicated occurrence of Na-carbonates in addition to (or instead of) Mg-carbonates (Carrozzo et al., 2017; Palomba et al., 2017).

The 3.4 μm band can be affected by other carriers, too. This is evident in the Ernutet crater (52°N, 45°E), where the 3.4 μm band is deeper than expected, and has been ascribed to the occurrence of organics (De Sanctis et al., 2017a).

The two Occator faculae are other peculiar regions due to their high albedo. They show a composition dissimilar from the rest of Ceres, with different types of phyllosilicates (Al-phyllosilicates instead of Mg- ones) and carbonates (Na-carbonates instead of Mg one), as well as with different relative abundance among components (De Sanctis et al., 2016; Palomba et al., 2017; Raponi et al., 2017a).

In order to obtain more detailed information about Ceres, its surface has been divided into 15 quadrangles (Williams et al., 2017; McCord and Zambon, 2017), which are currently being analyzed from both geological and mineralogical points of view.

This work focuses on the mineralogical mapping of the Occator quadrangle, spanning from latitude 22°S to 22°N and from longitudes 216°E to 288°E. This quadrangle is geologically variegated (Buczkowski et al., 2017). It is characterized by recent craters, superimposed on old cratered terrain, i.e. Occator (20°N 240°E), Azacca (6°S 219°E), Lociyo (6°S 228°E), and Nepen (7°N 222°E). Terrains at southern latitudes (i.e. below 10°S) and at eastern longitudes (i.e. eastward of 270°E) of the quadrangle include ejecta coming from impact generating the Urvara and Yalode craters, located in the homonymous quadrangles southward of Occator (Longobardo et al., 2017b).

From the data described in Section 2, we extracted the spectral parameters defined in Section 3 and mapped them on the quadrangle area (Section 4). Section 5 focuses on particular features of the quadrangle and in Section 6 conclusions are given.

2. Data

Here we use data from the Visible and InfraRed (VIR) mapping spectrometer. The instrument is characterized by a single optical head, including a visible (0.2–1 um) and an infrared (1–5 um) channel. The spectral sampling is 1.8 nm for the visible and 9.5 nm for the infrared channel (De Sanctis et al. 2011). VIR products are hyperspectral images, i.e. bi-dimensional spatial images (the two dimensions are referred to as samples and lines) acquired simultaneously at different wavelengths.

All the VIR spectra considered in this work have been calibrated in reflectance (I/F) (Filacchione and Ammannito, 2014), then procedures to remove spectral artifacts (Carrozzo et al. 2016) and the thermal emission (Raponi et al., 2017a) have been applied. Spectral artifacts were recognized and removed by obtaining an artifacts matrix, given by the residual of the spectrum extracted from each sample with respect to the sample average. The thermal contribution is removed by modeling the spectrum as the sum of a solar reflected radiance contribution and a Planck function, and then by subtracting the latter.

Two approaches of photometric corrections have been adapted onto VIR data (Ciarniello et al. 2017; Longobardo et al., 2017a), giving similar results. The photometric correction by Ciarniello et al. (2017) is obtained by applying the Hapke's model (Hapke, 2012) and is considered in this work. Moreover, the study by Longobardo et al. (2017a), based on a semi-empirical approach, demonstrated that the phase function of the Ceres average gives reliable results even when applied in the brightest spots of the surface, such as the Occator faculae.

The Dawn mission on Ceres is divided in different stages, characterized by different spacecraft altitude and hence different VIR spatial resolution, i.e. Approach (decreasing altitude and increasing resolution until the orbit stabilization), Rotation Characterization (altitude ~13,000 km and resolution ~3400 m/pixel), Survey (altitude ~4400 km and resolution ~1100 m/pixel); High Altitude Mapping Orbit (HAMO – altitude ~1470 km and resolution 360–400 m/pixel); Low Altitude Mapping Orbit (LAMO – altitude ~385 km and resolution 90–110 m/pixel). In order to obtain both good spatial coverage and spatial resolution, we consider here spectra acquired during the HAMO phase of the mission (Russell and Raymond, 2011).

3. Tools

The global mineralogy of the quadrangle is studied by means of the main spectral parameters maps describing the Ceres' spectrum, i.e. reflectance at 1.2 μm and 30° phase, strength of absorption bands at 2.7 μm (due to phyllosilicates) and 3.1 μm (due to ammonium), and the spectral slope between 1.2 μm and 1.9 μm.

According to the definition by Clark and Roush (1984), band depths were calculated as $1 - R_c/R_{con}$, being R_c and R_{con} the measured reflectance and the continuum at the band center (i.e. the band minimum after the continuum removal) wavelength. The continuum are defined as the straight lines between 2.63 μm and the local maximum in the 2.91–3.01 μm range (for the 2.7 μm band), and between the local maxima calculated in the 2.91–3.01 μm and 3.19–3.24 μm spectral ranges (for the 3.1 μm band).Spectral slope is defined as $(R_{1.891} - R_{1.163})/R_{1.891}(1.891 - 1.163)$, where R_λ is the reflectance at the wavelength λ. Details on the retrieval of these parameters are given by Frigeri et al. (this issue).

All the parameters are defined in a spectral range, where the thermal emission, which is observed at wavelength longer than 3.2 μm (Raponi et al., 2017b), is null or negligible, and hence their retrieval is not affected by the procedure of thermal removal.

The centers of the 2.7 μm and 3.1 μm bands do not show any variability on Ceres' surface (Ammannito et al. 2016), except for some specific locations (e.g., Occator crater), thus we do not show them in this paper. The two carbonates band depths (i.e. 3.4 μm and 4.0 μm absorption bands) also are quite uniform, except in localized regions, often corresponding to bright spots (Carrozzo et al., 2017; Palomba et al., 2017; Stein et al., 2017). We will discuss these particular cases for the regions located inside the Occator quadrangle.

4. Global maps

The Occator quadrangle maps of infrared 1.2 μm reflectance at 30° phase, band depth at 2.7 μm and band depth at 3.1 μm, and spectral slope are shown in Figs. 1, 2, 3 and 4, respectively.

In terms of these distributions, the Occator quadrangle follows a trend similar to the rest of the Ceres' surface, with albedo uncorrelated with the two band depths and the two band depths moderately correlated (Ammannito et al., 2016). We evaluated the correlation by calculating the Pearson coefficient ρ_{FB}, defined as $\sigma_{FB}/\sigma_F\sigma_B$ (where σ_F, σ_B and σ_{FB} are the variance of the two sets of parameters and their covariance, respectively) and already used in the spectral analysis of planetary surfaces (e.g. Palomba et al., 2015). It ranges between −1 (i.e. perfect anti-correlation) and 1 (i.e. perfect correlation), whereas a zero value means lack of correlation.

In the Occator quadrangle case, ρ_{FB} is almost zero between albedo and each band depth, whereas is about 0.3 between the two band depths, corresponding to moderate correlation (Fig. 5).

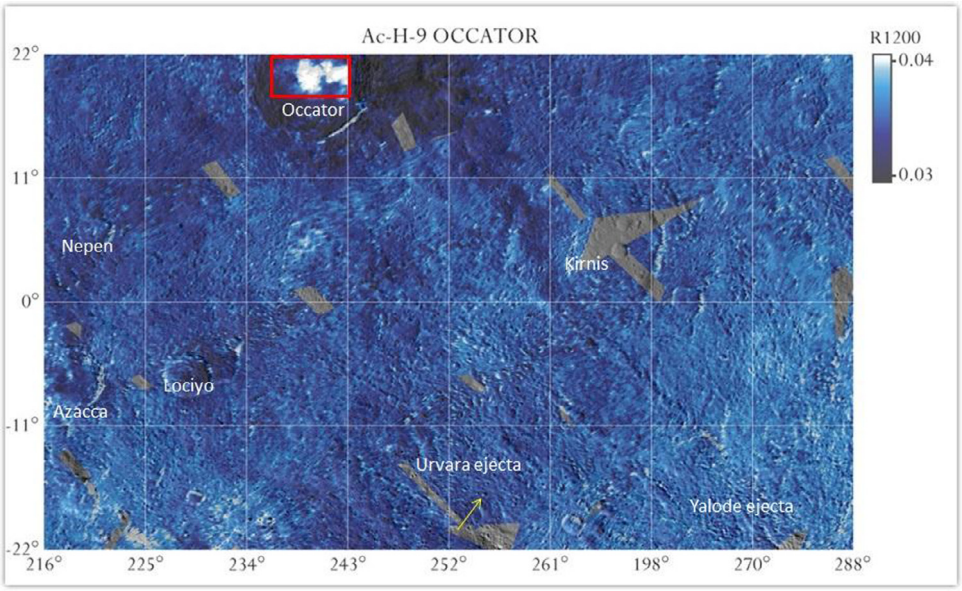

Fig. 1. Map of 1.2 μm reflectance at 30° phase of the Occator quadrangle, superimposed on the Framing Camera (FC) mosaic with a transparence of 25%. Gray means no VIR coverage. The red square encloses the Occator faculae region, shown in Fig. 6, whereas the arrow indicates the location of the B46 bright spot (small-scale feature).

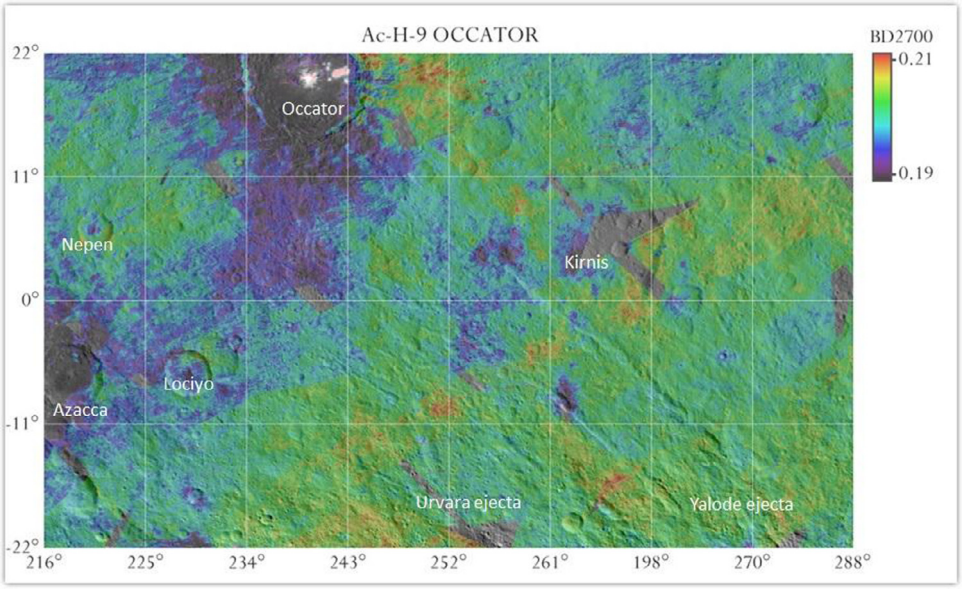

Fig. 2. Band depth at 2.7 μm of the Occator quadrangle, superimposed on the Framing Camera (FC) mosaic with a transparence of 25%. The FC mosaic is fully visible in absence of VIR coverage or when band depth values are out of the color scale.

The inferred behavior is an association between ammoniated and hydrated materials.

With the exception of the two faculae located in the Occator crater, the albedo distribution is quite uniform (the geometric albedo standard deviation is 0.001), with a slight longitudinal distribution, since eastern terrains are faintly brighter. The darkest terrains of the quadrangle correspond to the Occator floor (excluding faculae) and eastern ejecta, which are among the darkest features of Ceres.

Band depths show instead a latitudinal distribution, being generally shallower at northern latitudes (with exception of the Occator eastern ejecta) and deeper in the southern-eastern part of the quadrangle. This region corresponds to Urvara and Yalode ejecta (Buczkowski et al., 2017), and hence an association between geology and mineralogy arises. The shallowest band depths are instead observed in correspondence with craters, i.e. Occator, Lociyo, Azacca and Nepen, and, to a lesser extent, Kirnis (5°N 265°E). A general anti-correlation between age and band depth is observed for Ceres' craters (Stephan et al., 2017a), and the craters in this quadrangle do follow this trend, since Occator, Azacca and Lociyo are the youngest and showing the shallowest band depths. According to the Lunar Derived Model (Schmedemann et al., 2014), the ages of these craters is in fact lower than ~80 Ma, and in particular is ~20 Ma for Occator (Stephan et al., 2017a and references therein); Nepen is slightly older, whereas Kirnis is the oldest craters of the quadrangle (Buczkowski et al., 2017).

This behavior can be ascribed to a temporal variation of properties affecting these bands, such as the abundance of ammoniated phyllosilicates, or physical properties, such as grain size of one or more end members. This temporal variation could be due to terrains mixing, or to space weathering, causing fragmentation of coarse grains and hence reducing the average grain size (Stephan et al. 2017b).

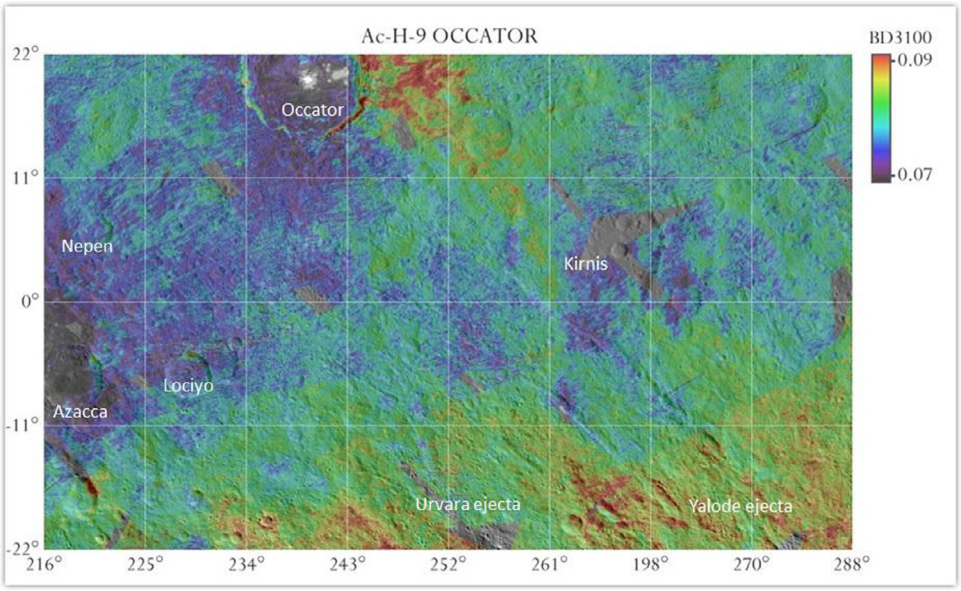

Fig. 3. Band depth at 3.1 μm of the Occator quadrangle, superimposed on the Framing Camera (FC) mosaic with a transparence of 25%. The FC mosaic is fully visible in absence of VIR coverage or when band depth values are out of the color scale.

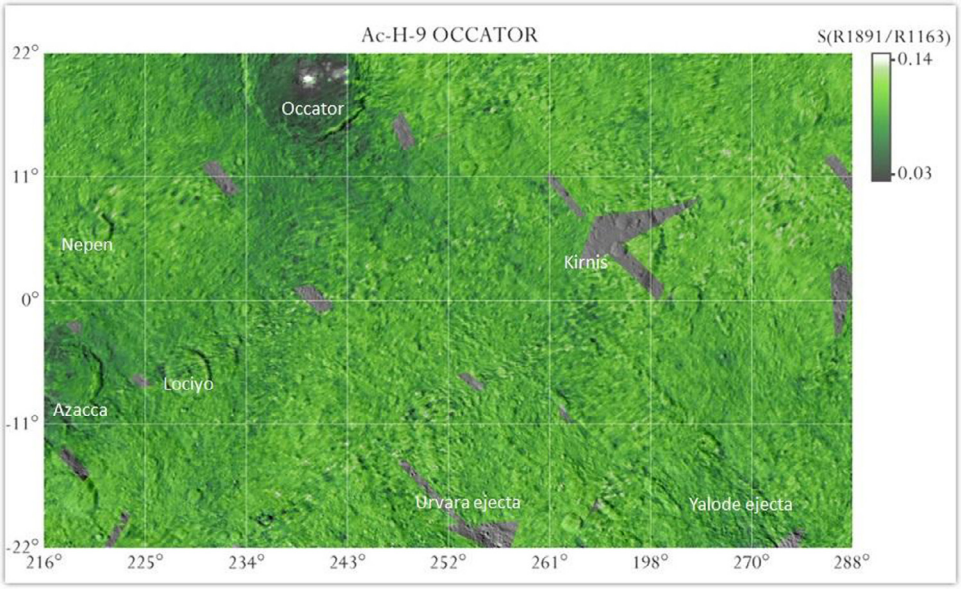

Fig. 4. Infrared slope of the Occator quadrangle, superimposed on the Framing Camera (FC) mosaic with a transparence of 25%. The FC mosaic is fully visible in absence of VIR coverage or when slope are values out of the mapped color scale.

The spectral slope also shows its lowest values in correspondence of the Occator crater, and southern and eastern ejecta, i.e. between 0.03 and 0.05. In particular, the faculae's slope takes negative values and is outside the color scale mapped in Fig. 4 (we see the FC map, only, in correspondence of the faculae). The spectral slope of the Azacca crater ranges between 0.05 and 0.07, and is also lower than the quadrangle average (i.e. 0.09).

5. Main features

5.1. Occator

5.1.1. Faculae

Cerealia (19°N 239°E) and Vinalia (20°N 242°E) faculae are the brightest regions of the Ceres surface with an average 1.2 μm reflectance at 30° of phase angle of 0.08 and 0.062, respectively (Palomba et al., 2017). Their location in the quadrangle is highlighted in Fig. 1. They are characterized by a large amount of carbonates (i.e., 30–40%, De Sanctis et al., 2016), as inferred by the deeper bands at 3.4 and 4.0 μm and the broader 3.4 μm band (Fig. 6). Moreover, the longward shift of the 4.0 μm band center from 3.95 μm (Ceres average) to 4.0 μm (Occator faculae) indicates the occurrence of sodium carbonate, instead of calcium and magnesium carbonates, as for the rest of Ceres surface. The morphological analysis by Stein et al. (2017) concluded that the most plausible scenario for formation of carbonate-rich faculae is that the impact forming the Occator crater caused upwelling of extant subsurface brines.

The common behavior of bright spots on Ceres is a general anti-correlation between the carbonate (3.4 μm and 4.0 μm) and the ammoniated phyllosilicates (2.7 μm and 3.1 μm) band depths (Palomba et al., 2017). The Occator faculae follow this behavior for

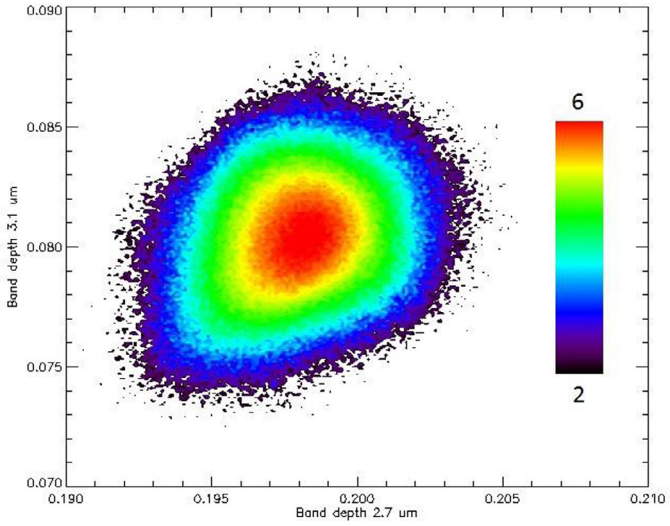

Fig. 5. Density plot correlating the two band depths at 2.7 μm and 3.1 μm on the Occator quadrangle. The color shows the logarithm of the number of observations.

what concerns band depth at 3.1 μm which is indeed very low (i.e. 0.02–0.03, below the minimum value mapped in Fig. 3). On the other hand, the 2.7 μm band depth is much larger than expected for a carbonate-rich area (Palomba et al. 2017). The band center shifts from 2.72 μm (Ceres average) to 2.76 μm (Occator faculae), indicating the occurrence of Al-phyllosilicates instead of Mg-phyllosilicates (De Sanctis et al., 2016). The presence of this kind of phyllosilicate is another peculiarity of these faculae and explains the deepening of the 2.7 μm band despite the presence of carbonates.

5.1.2. Floor

The Occator floor is very dark, with very shallow bands at 2.7 μm and 3.1 μm (i.e. down to 0.19 and 0.07, respectively), and with a very low spectral slope (i.e. down to 0.03). This represents a rare case of correspondence between low values of all these spectral parameters. Moreover, the carbonate bands are shallow, too (Carrozzo et al, 2017). The low values of albedo (reflectance at 1.2 μm of 0.03), as well as the 3.4 and 4.0 μm band depths, suggest that there is no depletion of ammoniated phyllosilicates due to formation of carbonates, and therefore the shallowing of 2.7 μm and 3.1 μm band depths should be ascribed to other effects. We observe that this shallowing reflects the general anti-correlation trend between crater age and these band depths, which may be ascribed to different regolith physical properties, e.g. a larger grain size. Larger granulometry enhances the regolith shadowing, causing an albedo decreasing (Hapke, 1981; Longobardo et al., 2014), and has been discussed lowering the spectral slope (Stephan et al., 2017b; Cloutis et al., 2011). Both these behaviors are indeed observed on the Occator floors, corroborating our hypothesis.

The shallowing of ammoniated phyllosilicate bands as well as the flattening of the spectral slope are not observed on the crater rim, which corresponds to talus material, i.e. a different geological unit (Buczkowski et al., 2017). Talus is a slope formed by an accumulation of broken rock debris (observed also on other asteroids, e.g. Williams et al., 2014), and its larger band depths could be ascribed to a different physical state (i.e. loose material instead of hard material).

5.1.3. Ejecta

Ejecta around Occator crater have two different spectral behaviors: southern and western ejecta have a 1.2 μm reflectance at the 30° phase comparable to the Ceres average (e.g., 0.035), very shallow 2.7 μm and 3.1 μm band depths, and spectral slope about 50% lower than surroundings. Otherwise, eastern ejecta are dark (reflectance of 0.032) and show the deepest ammoniated phyllosilicates bands in the quadrangle. They extend down to the lower boundary of the quadrangle, superimposing on the Kirnis crater and the Urvara ejecta, indicating that they have been generated by an event more recent than formation of these craters, according to its geological classification (Buczkowski et al., 2017).

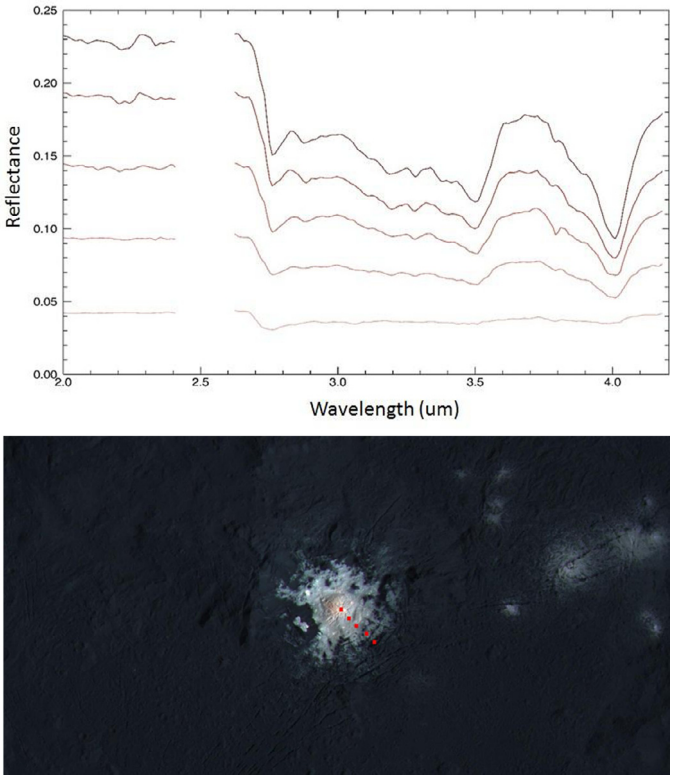

Fig. 6. *Top.* Spectra from Cerealia Facula (top, the brightest one) down to facula surroundings, i.e. Occator floor (bottom, the darkest one). At increasing reflectance, the bands at 3.4 μm and 4.0 μm, ascribed to carbonates, are clearer, and the 2.7 μm band remains high, too, due the occurrence of Al-phyllosilicates. The 3.1 μm band is instead almost absent. In the facula spectrum band center of the phyllosilicates and carbonates bands are longward shifted with respect to their surroundings (from 2.72 to 2.76 μm and from 3.95 to 4.0 μm, respectively), indicating a different composition of these phases. *Bottom*: Framing Camera image corresponding to the region enclosed in the square in Fig. 1. The filled squares indicates the locations of the spectra shown in the top figure.

Distribution of 4.0 μm band depth (Carrozzo et al., 2017) shows that carbonates occur in southern and western ejecta, which could partially explain the different spectral properties with respect to eastern ejecta.

Comparison with the geological map (Buczkowski et al., 2017; Williams et al., 2017) indicates that “dark” and “bright” ejecta belong to two different geological features and hence had a different formation, evolution or age. In particular, dark ejecta could be associated with the unnamed crater north of the Occator crater, located in the Ezinu quadrangle (Combe et al., 2017): the fact that the southern rim of this crater is covered by the Occator’s northern rim (Fig. 7) indicates that this crater is older than Occator itself. Therefore, the different spectral properties between dark and bright ejecta may be associated with the different impact or post-impact processes subjected from the two craters.

5.2. Azacca

The Azacca crater is characterized by very low band depths (down to 0.19 and 0.07 for the 2.7 and 3.1 μm band depth, respec-

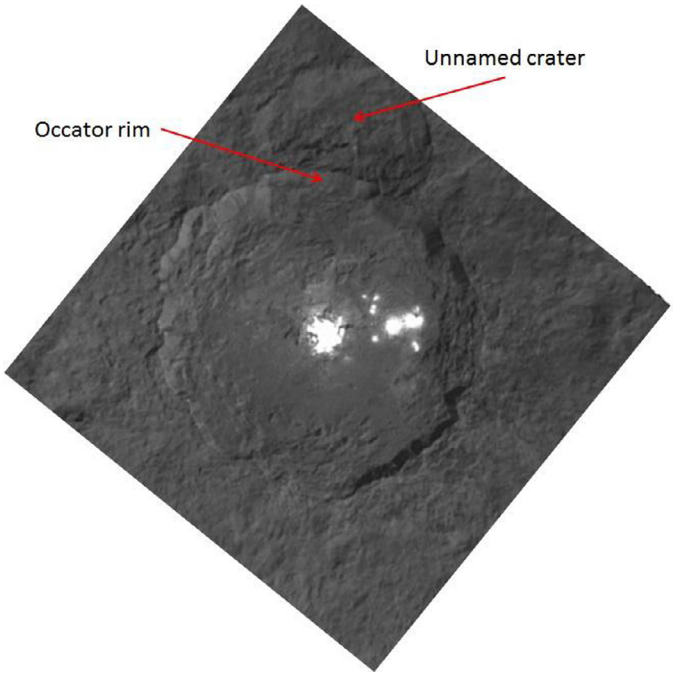

Fig. 7. Occator rim superimposed on the northern unnamed crater (FC image).

tively) on both floor and ejecta, with the exception of the eastern rim where band depths increase. The albedo distribution is uncorrelated with the 2.7 μm and 3.1 μm absorption features, with brightest patches associated with the northern rim and wall, central peak and SW ejecta.

The low band depths would be justified by the overall anticorrelation between age and band depths, which, in turn, may be ascribed to different physical properties of the regolith, as inferred also by the changing spectral slope. The brightest areas in and around the crater are associated with the occurrence of Na-carbonates (Carrozzo et al., 2017), which could explain their higher albedo. The higher band depth areas in the eastern rim of the crater correspond to a different geological feature, i.e., talus material. Because no band center variations are observed in correspondence of this unit, talus' composition is the same as the rest of the crater, therefore its different band depth could be due to a change of physical state (i.e. loose material instead of hard material).

5.3. Lociyo and Nepen

These two craters have similar spectral behavior, i.e. shallow bands in the floor and central peak, and band depths 10–20% higher in correspondence with the tali on the crater walls. Albedo distribution is instead independent of band depth. The band depth shallowing on the floor is common to the other young craters of the quadrangle (Occator and Azacca, see Fig. 5), whereas the deepening in correspondence of tali, still observed in Occator and Azacca, may indicate different physical properties.

5.4. Urvara and Yalode ejecta

The Urvara and Yalode ejecta are superimposed on the old cratered terrain which is the dominant feature of the quadrangle. They are recognizable by deeper band depths than the equatorial cratered terrain. This can be ascribed to the fact that they originated from the Southern Hemisphere, where the abundance of ammoniated phyllosilicates is generally higher (Ammannito et al., 2016; Longobardo et al., 2017b; De Sanctis et al., 2017b).

A slight albedo increase (up to 10%) is associated with Yalode ejecta but not with Urvara ejecta: this can be ascribed to the different composition or physical properties of the terrains where the impacts generating the two craters occurred, as supported by the different distribution of spectral parameters in the Urvara and Yalode craters, with Urvara showing deeper absorption bands (Longobardo et al., 2017b).

5.5. Bright spots

In addition to the two faculae, another bright spot has been identified in the Occator quadrangle. According to the definition of Palomba et al. (2017), an area is considered a "bright spot" when its albedo is at least 30% larger than its surroundings. The feature in the Occator quadrangle satisfying this requirement is labeled by Palomba et al. (2017) as B46 (16.5°S 255°E). It is small-scale spot associated with a crater rim, and is located in the terrains superimposed by Urvara ejecta, in particular where the Occator ejecta overlap the Urvara ones. The spot position is highlighted with an arrow in Fig. 1 (where it is not recognizable, due to its small extension).

It shows albedo and depths similar to most of the bright spots, is not associated to band center change and hence has a composition similar to the rest of Ceres, i.e. opaques, ammoniated clays and Ca-Mg carbonates. Its brightening could be justified by a lower amount of opaques, by different physical properties or to the occurrence of material coming from the Occator crater.

6. Conclusions

We mapped the distribution of the reflectance at 1.2 μm, 2.7 μm and 3.1 μm band depths and infrared spectral slope in the Occator quadrangle of Ceres, which is bounded by latitudes 22°S to 22°N and longitudes 214°E and 288°E. We find for this quadrangle that variation in the two band depths are correlated with each other but not with albedo. These findings are in agreement with behavior overmost of Ceres' surface. In addition, the brighter areas, found in association with Occator faculae, are due to sodium carbonates deposited upon younger terrains, but one less-bright area is deposited on older terrain, suggesting either an aging effect for the bright material or a difference in the deposits formed in older terrain.

There is an overall correlation between mapped geological units and spectral parameter distribution, contrary to that observed for Vesta (Longobardo et al., 2015). In particular, young craters are associated with a shallower band depths, as is common behavior across Ceres. This behavior could be caused by different regolith physical properties (e.g., grain size) or differences in the abundance of dark materials mixed with ammoniated clays. We also observe a flattening of the spectral slope (less red) at these craters. De Sanctis et al. (2015) showed that the dark materials on Ceres have redder spectral slope than the ammoniated phyllosilicates, therefore a greater amount of dark material would produce a spectral slope increase, and Cloutis et al. (2011) showed that for dark meteorites, the coarser samples have less red spectral slopes than for finer samples, both results suggesting that grain size differences are responsible for the younger crater spectral behavior.

Two types of ejecta are observed around the Occator crater that differ in albedo and the band depths and spectral slope. The different spectral behavior is associated with their belonging to different geological units, and probably is due to a different formation history.

The Urvara and Yalode ejecta, located in the southern region of the quadrangle, clearly show greater band depths and brighter reflectance than do the terrains they overlap, due to their origin from a different terrain.

Finally, tali in crater rims and walls show increased band depths compared with surrounding material, indicating a difference in physical state.

In general, the spectral characteristics of this quadrangle are similar to those found over most of Ceres' surface except for the Occator Crater region.

Acknowledgments

VIR is funded by the Italian Space Agency-ASI and was developed under the leadership of INAF-Istituto di Astrofisica e Planetologia Spaziali, Rome–Italy. The instrument was built by Selex-Galileo, Florence-Italy. The authors acknowledge the support of the Dawn Science, Instrument, and Operations Teams.

The FC Team is thanked for sharing their images.

Sharon Uy (UCLA, USA) is thanked for the manuscript revision.

References

Ammannito, E., et al., 2016. Distribution of phyllosilicates on the surface of Ceres. Science 353, 6303. doi:10.1126/science.aaf4279.

Buczkowski, D.H., et al., 2017. The geology of the Occator quadrangle of dwarf planet Ceres: Floor-fractured craters and other geomorphic evidence of cryomagmatism. Icarus, in press doi:10.1016/j.icarus.2017.05.025.

Carrozzo, F.G., et al., 2016. Artifacts reduction in VIR/Dawn data. Review of Scientific Instruments 87, 12. doi:10.1063/1.4972256.

Carrozzo, F.G. et al., 2017. Nature, formation and distribution of Carbonates on Ceres, Sci. Adv. Under Review.

Ciarniello, M., et al., 2017. Spectrophotometric properties of dwarf planet Ceres from VIR onboard Dawn mission. Astron. Astrophys. 598, A130.

Clark, R.N., Roush, T.L., 1984. Reflectance spectroscopy: quantitative analysis techniques for remote sensing applications. J. Geophys. Res. 89 (B7), 632–6340.

Cloutis, E.A., et al., 2011. Spectral reflectance properties of carbonaceous chondrites: 1. CI chondrites. Icarus 212 (1), 180–209.

Combe, J.-P. et al., 2017. The Surface Composition of Ceres Ezinu quadrangle analyzed by the Dawn mission, Icarus (submitted for publication).

De Sanctis, M.C., et al., 2011. The VIR Spectrometer. Space Sci. Rev. 163, 329–369.

De Sanctis, M.C., et al., 2015. Ammoniated phyllosilicates with a likely outer System origin on (1) Ceres. Nature 528, 241–244.

De Sanctis, M.C., et al., 2016. Bright carbonate deposits as evidence of aqueous alteration on (1) Ceres. Nature 536, 54–57.

De Sanctis, M.C., et al., 2017a. Localized aliphatic organic material on the surface of Ceres. Science 355 (6326), 719–722.

De Sanctis, M.C. et al. 2017b. Ac-H-11 Sintana and Ac-H-12 Toharu quadrangles: Assessing the large and small scale heterogeneities of Ceres' surface, Icarus, in press 2017, https://doi.org/10.1016/j.icarus.2017.08.014.

Filacchione, G. and Ammannito, E. (2014), Dawn VIR calibration document Version 2.4, https://sbn.psi.edu/archive/dawn/vir/DWNVVIR_I1B/DOCUMENT/VIR_CALIBRATION/VIR_CALIBRATION_V2_4.PDF.

Hapke, B., 1981. Bidirectional reflectance spectroscopy. I – Theory. J. Geophys. Res. 86, 3039–3054.

Hapke, B., 2012. Theory of Reflectance and Emittance Spectroscopy. Cambridge University Press.

Longobardo, A., et al., 2014. Photometric behavior of spectral parameters in Vesta dark and bright regions as inferred by the Dawn VIR spectrometer. Icarus 240, 20–35.

Longobardo, A., et al., 2015. Mineralogical and spectral analysis of Vesta's Gegania and Lucaria quadrangles and comparative analysis of their key features. Icarus 259, 72–90.

Longobardo, A. et al., 2017a. Photometry of Ceres and Occator faculae as inferred by VIR/Dawn data, Icarus (submitted for publication).

Longobardo, A. et al. 2017b. Mineralogy of the Urvara-Yalode region on Ceres, Icarus (submitted for publication).

McCord, T.B. and Zambon, F., 2017. The surface composition of Ceres from the Dawn mission, Icarus (submitted for publication).

Palomba, E., et al., 2015. Detection of new olivine-rich locations on Vesta. Icarus 258, 120–134.

Palomba, E. et al., 2017. Compositional differences among Bright Spots on the Ceres surface, Icarus, in press, doi: 10.1016/j.icarus.2017.09.020.

Raponi, A. et al. 2017a. Mineralogical mapping of Ac-H-2 'Coniraya' quadrangle, Icarus (submitted for publication).

Raponi, A. et al. 2017b. Mineralogy of Occator crater on Ceres, Icarus (submitted for publication).

Russell, C.T., Raymond, C.A., 2011. The Dawn Mission to Vesta and Ceres. Space Sci. Rev. 163 (1-4), 3–23.

Schmedemann, N., et al., 2014. The cratering record, chronology and surface ages of (4) Vesta in comparison 39 to smaller asteroids and the ages of HED meteorites. Planetary Space Sci. 103, 104–130.

Sierks, H., et al., 2011. The dawn framing camera. Space Sci. Rev. 163, 263–327.

Stein, N. et al., 2017. Characteristic, Formation and Evolution of Faculae (Bright Spots) on Ceres, Icarus, Under Review.

Stephan, K. et al., 2017a. Ceres' craters – Relationships between surface composition and geology, Icarus, Under Review.

Stephan, K., et al., 2017b. An investigation of the bluish material on Ceres. Geophys. Res. Lett. 44 (4), 1660–1668.

Williams, D., et al., 2014. Lobate and flow-like features on asteroid Vesta. Planetary Space Sci. 103, 24–35.

Williams, D., et al., 2017. Introduction: The geologic mapping of Ceres. Icarus, in press doi:10.1016/j.icarus.2017.05.004.